Self-Assembly of Stimuli-Responsive Water-Soluble [60]Fullerene End-Capped Ampholytic Block Copolymer

P.Ravi, S. Dai and K. C. Tam*
Singapore-MIT Alliance, School of Mechanical and Production Engineering, Nanyang Technological University, Singapore-639798

Abstract: **Well-defined, water-soluble, pH and temperature stimuli-responsive [60]fullerene (C_{60}) containing ampholytic block copolymer of poly((methacrylic acid)-*block*-(2-(dimethylamino)ethyl methacrylate))-*block*–C_{60} (P(MAA-*b*-DMAEMA)-*b*-C_{60}) was synthesized by the atom transfer radical polymerization (ATRP) technique. The self-assembly behaviour of the C_{60} containing polyampholyte in aqueous solution was characterized by dynamic light scattering (DLS), and transmission electron microscopy. This amphiphilic mono-C_{60} end-capped block copolymer shows enhanced solubility in aqueous medium at room and elevated temperatures and at low and high pH but phase-separates at intermediate pH of between 5.4 and 8.8. The self assembly of the copolymer is different from that of P(MAA-*b*-DMAEMA). Examination of the association behavior using DLS revealed the co-existence of unimers and aggregates at low pH at all temperatures studied, with the association being driven by the balance of hydrophobic and electrostatic interactions. Unimers and aggregates of different microstructures are also observed at high pH and at temperatures below the lower critical solution temperature (LCST) of PDMAEMA. At high pH and at temperatures above the LCST of PDMAEMA, the formation of micelles and aggregates co-existing in solution is driven by the combination of hydrophobic, electrostatic, and charge-transfer interactions.**

Index Terms. **Ampholytic, Fullerene, Self-assemble, Stimuli-responsive**

I. Introduction

Despite the discovery of potential applications of fullerenes in biological systems, the insolubility of fullerenes in water and organic solvents has hindered its progress in this field of research[1]. The solubility of fullerenes can be enhanced through the formation of charge-transfer complexes with organic compounds possessing electron-donating properties[2],[3]. In addition, their solubility can also be enhanced by functionalizing the fullerenes with hydrophilic compounds. These compounds are usually either water-soluble groups such as alcohols[4], carboxylic acids[5], and amines[6], or long-chain hydrophilic polymers[7],[8]. These amphiphilic fullerene derivatives self-assemble into interesting nano-scale structures in water, which have a variety of potential applications[9]. For example, Sitharaman et al. recently studied the aggregation properties of tris-malonic acid-C_{60} (C_3) as a function of temperature, concentration and pH in aqueous solution. They reported that C_3 could form nanocrystalline aggregates under physiological conditions, which are actively being pursued as a prime drug candidate for various neurological diseases, as well as for possible lifespan extension [10].

To date, mono-substituted fullerenes with well-defined polymers have been synthesized and their solution behaviour examined since these polymers retain the unique fullerene properties and may have potential biological applications. For example, micelle-like core-shell aggregates with shells containing highly-stretched polymer chains were reported for PMMA-*b*-C_{60} and P*n*BMA-*b*-C_{60} systems in THF [11]. Song et al. reported large spherical aggregates for single- and two-arm fullerene-containing poly(ethylene oxide)s in THF and aqueous solution [12],[13]. Although the above polymers were synthesized by cycloaddition reaction of azide-terminated polymers with fullerene, the atom transfer radical polymerization (ATRP) technique has recently been used to synthesize well-defined fullerene-containing polymers. For instance, Zhou and co-workers employed this technique to synthesize well-defined fullerene-containing polystyrene and poly(methyl methacrylate) [14]. The well-defined di- and tetra-adducts of polystyrene-C_{60} have been synthesized using ATRP by Audouin et al [15]. In addition, ATRP was also employed to synthesis the well-defined poly(*tert*-butyl acrylate-*b*-styrene)-C_{60} for photoconductive applications [16]. The water-soluble C_{60}-containing poly(acrylic acid) (PAA-*b*-C_{60}) synthesized by Yang et al. formed core-shell micelles in aqueous solution, which enhanced the photoconductivity of films [17]. Recently, we synthesized C_{60}-containing well-defined water-soluble C_{60} containing polymer systems using ATRP. Poly(methacrylic acid)-*b*-C_{60} (PMAA-*b*-C_{60}) and poly(2-(dimethylamino)ethyl methacrylate)-*b*-C_{60} (PDMAEMA-*b*-C_{60}), and their self-assembly behavior in aqueous solution was studied as a function of pH and temperature[18], [19].

Manuscript received November 18, 2004. This work was supported by Singapore-MIT Alliance, Singapore.

F.A. is with Singapore-MIT Alliance, School of Mechanical and production Engineering, Nanyang Technological University, Singapore-639798, e-mail: ravi@ntu.edu.sg

S.A. is with Singapore-MIT Alliance, School of Mechanical and production Engineering, Nanyang Technological University, Singapore-639798, e-mail: msdai@ntu.edu.sg

T.A. is with Singapore-MIT Alliance, School of Mechanical and production Engineering, Nanyang Technological University, Singapore-639798. Corresponding author phone: 67905590; fax: 67924062; e-mail: mkctam@ntu.edu.sg.

Stimuli-responsive block copolymers are an interesting class of block copolymers because their physical and chemical properties can be adjusted by external stimuli. For example, hydrophilic or hydrophobic properties can be induced by the variation of pH or temperature [20], [21]. This type of reversible change has far-reaching consequences on aggregation, phase behavior, and solubility, leading to widespread applications in drug delivery systems[22], in devices as actuators [23], artificial muscles, and controlled molecular gates and switches [24] Studies conducted on the stimuli-responsive drug-release behavior of block copolymers have demonstrated their possible applications [25], [26]. Since PMAA and PDMAEMA are proven to be stimuli-responsive and biocompatible [27], studies have been conducted on P(MAA-*b*-DMAEMA) block copolymers by a few groups. Gohy et al. investigated the association behavior of a series of mono-dispersed P(MAA-*b*-DMAEMA) ampholytic diblock copolymers in water in the dilute regime as a function of pH and concentration [28]. For copolymers containing a major PDMAEMA block, they formed spherical micelles below the isoelectric point (IEP) but are insoluble at and above the IEP. For copolymers containing a minor PDMAEMA block, they formed spherical micelles and complex aggregates below and above the IEP respectively but are insoluble at and around the IEP. Lowe et al. synthesized P(MAA-*b*-DMAEMA) copolymers by group transfer polymerization and examined their aqueous micellization properties using dynamic light scattering (DLS) and variable temperature ^{1}H-NMR spectroscopy [29]. For a P(MAA-*b*-DMAEMA) copolymer containing 57 mol% MAA, they found unimers at 25 °C but large aggregates at elevated temperatures in alkaline solution both in the absence and presence of salt.

The self-assembly of PAA-b-C_{60}, PMAA-*b*-C_{60} and PDMAEMA-*b*-C_{60} have been studied as a function of pH. Since the polyampholytes always exhibit antipolyelectrolyte effect, the solution behavior of C_{60}-containg polyampholytes is unexplored. Due to the interesting stimuli-responsive self-assembly of P(MAA-*b*-DMAEMA), the well-defined ampholytic C_{60}-containing P(MAA-*b*-DMAEMA) (P(MAA-*b*-DMAEMA)-*b*-C_{60}) was synthesized using the ATRP technique and its pH- and temperature-responsive aggregation behaviour in dilute aqueous solution was examined in detail.

II. Experimental Section

A. Materials.

C_{60} (99.9%) was obtained from Materials Technologies Research (MTR) Ltd. 2-(dimethylamino)ethyl methacrylate (DMAEMA), tert-butylmethacrylate (tBMA), CuCl (99.995%), and 1,1,4,7,10,10-hexamethyltriethylenetetramine (HMTETA, 97%) were obtained from Aldrich and used without further purification. The monomers were purified by passing through a basic alumina column, dried over CaH_2, and distilled under reduced pressure. All solvents were freshly distilled before use.

B. Synthesis of P(tBMA-b-DMAEMA)-Cl Macroinitiator.

All synthetic steps were carried out under an argon atmosphere. First, the well-defined –Cl terminated PtBMA macroinitiator (M_n = 14,500 Da & M_w/M_n = 1.13) was synthesized as described in our previous paper [9]. To a Schlenk flask, a known amount of PtBMA-Cl, CuCl (molar equivalent to PtBMA), DMAEMA monomer, and anisole (1:1 volume ratio to monomer) were introduced. The reaction mixture was degassed three times using freeze-pump-thaw cycles. The degassed ligand (HMTETA, molar equivalent to PtBMA) was introduced just before the final cycle and the flask was placed in a thermostated oil bath at 60 °C. When the reaction yield reached ~ 90 %, the reaction was stopped. The catalyst was removed using a basic alumina column and the polymer was recovered by precipitation in excess of cold n-hexane, filtered, and dried under vacuum. The reprecipitation process was repeated three times to remove the unreacted monomer and impurities.

C. *Synthesis of P(MAA-b-DMAEMA)-b-C_{60}.*

P(*t*BMA-*b*-DMAEMA)-Cl was charged into a Schlenk flask and dissolved in a small amount of 1,2-dichlorobenzene. In a separate Schlenk flask C_{60} (P(*t*BMA-*b*-DMAEMA)-Cl:C_{60} molar ratio of 1:3) and CuCl/HMTETA (1:1) catalyst system were dissolved in 20 mL of 1,2-dichlorobenzene. Three freeze-pump-thaw cycles were performed for both the Schlenk flasks. Finally, the macroinitiator was added into the catalyst complex via a double-tipped syringe and reacted for 24 h at 90 °C. After 24 h, the reaction mixture was diluted with THF. The catalyst was first removed using a basic alumina column and the solvent was then evacuated under vacuum. The unreacted C_{60} was removed by dissolving the polymer in THF, filtered and passed through the alumina column. The filtrate was concentrated and precipitated in excess amounts of cold *n*-hexane to yield a dark brown polymer. The procedure was repeated three times to ensure the complete removal of unreacted C_{60}. Subsequently, the *tert*-butyl groups of the P(*t*BMA) blocks were hydrolyzed with concentrated hydrochloric acid in dioxane at 85 °C for 6 hrs to form PMAA blocks and the block copolymer was precipitated in excess of *n*-hexane. The polymer was washed with *n*-hexane for several times and dried under vacuum. The fully hydrolyzed final product was confirmed by FT-IR (KBr-pellet) and potentiometric titration

C. Characterization

*1) Gel Permeation Chromatography***.** An Agilent 1100 series GPC system equipped with a LC pump, PLgel 5µm MIXED-C column, RI and RI/UV dual mode detectors was used to determine polymer molecular weights and polydispersities. The UV/RI (330 nm was used to monitor the signal) dual detector system was used to confirm the

grafting of C_{60} onto the polymer. The column was calibrated with narrow molecular weight polystyrene standards. HPLC grade THF stabilized with BHT was used as the mobile phase. The flow rate was maintained at 1.0 mL/min

2) NMR Spectroscopy. The ^{1}H-NMR spectrum of the precursor block copolymer was measured using a Brüker DRX400 instrument in $CDCl_3$.

3) Thermogravimetric Analysis. Thermogravimetric measurements were carried out with a Perkin-Elmer TGA 7 Thermogravimetric Analyzer. Known amounts of samples were heated from 25 to 850°C at a rate of 10°C/min in a dynamic nitrogen atmosphere.

4) UV-Visible Spectroscopy. Absorption measurements were made on copolymer solutions at 25 °C with concentrations ranging from 0.025 to 0.25 wt% using an Agilent 8453 UV-visible spectrophotometer at pH 3 and 11. Visible light transmittance measurements were carried out at 25 °C and 55 °C a wavelength of 600 nm on 0.3 wt% copolymer solutions.

5) Dynamic Light Scattering. Room temperature light scattering measurements were made with a Brookhaven BI-200SM goniometer equipped with a BI9000AT digital correlator. Intermediate and elevated temperature light scattering measurements were made with a Brookhaven ZetaPlus system equipped with temperature control unit. The inverse Laplace transformation of REPES in the GENDIST software package was used to obtain decay time distribution functions with the probability-to-reject set at 0.5. The copolymer concentrations ranged from 0.05 to 0.30 wt% in 0.1 M NaCl solution while the scattering angles were varied from 30 to 90°.

6) Transmission Electron Microscopy. For each transmission electron microscopic sample, a drop of dilute copolymer solution was placed onto a 200-mesh copper grid pre-coated either with carbon or Formvar. The samples were dried overnight before measurement using a JEOL JEM 2010 transmission electron microscope operating at an accelerating voltage of 200 kV.

III. Results and Discussion

Recently, well-defined poly(methyl methacrylate) and polystyrene have been successfully mono-end-capped with C_{60} using the ATRP technique [30]. The synthesis details for P(MAA-*b*-DMAEMA)-*b*-C_{60} are described in Scheme 1. Though the synthesis of P(MAA-*b*-DMA) has been reported using the group transfer polymerization technique [29 above this is the first time ATRP was used to synthesize the same block copolymer. Using the P*t*BMA-Cl as macroinitiator, DMA was block copolymerized in the presence of CuCl/HMTETA catalyst system in anisole at 60 °C. Fig. 1b shows the mono-modal GPC curve of P(*t*BMA-*b*-DMA). Using the P(*t*BMA-*b*-DMA)-Cl as macroinitiator, ATRP was used again to block the polymer to the C_{60} using the same catalyst system. The molar ratio of 1:3 (P(*t*BMA-*b*-DMA)-Cl:C_{60}) was used to avoid the multiple grafting of the polymer on C_{60}. The comparison of the GPC traces for P(*t*BMA-*b*-DMA)-*b*-C_{60} determined using different detectors (RI and RI/UV dual detectors) is shown in Figure 1c & 1d. The mono-modal GPC traces from the RI detector revealed that the molecular weight of the P(*t*BMA-*b*-DMA)-*b*-C_{60} polymer was 25,300 Da with M_w/M_n = 1.22. Based on the combination of ^{1}H-NMR and GPC traces, the degree of polymerization was determined to be P(tBMA$_{102}$-*b*-DMAEMA$_{67}$).

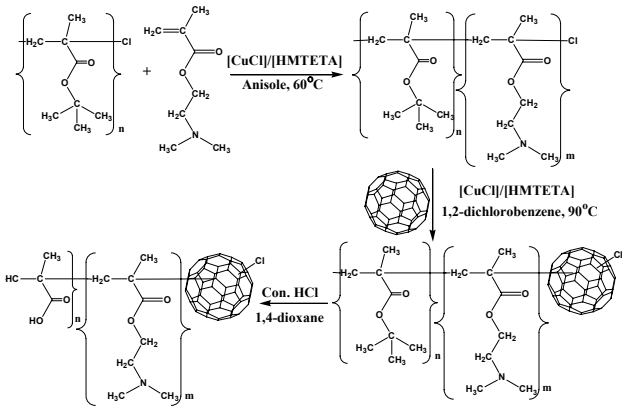

Scheme 1. Synthesis of C_{60} end-capped polyampholyte

Fig. 1. GPC traces of a) P(*t*BMA)-Cl, b) P(*t*BMA-*b*-DMA), c) P(*t*BMA-b-DMA)-*b*-C_{60} from RI detector, d) P(*t*BMA-*b*-DMA)-b-C_{60} from UV detector.

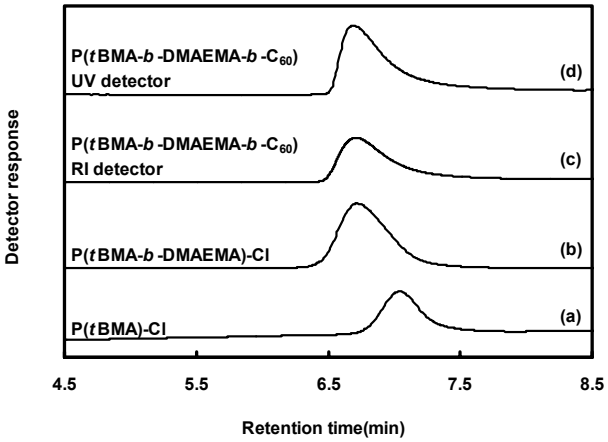

The absence of any tailing or multiple peaks confirmed the mono-substitution of the copolymer onto C_{60} molecules. Since only the polymers that contain C_{60} were detectable from both UV ($\lambda \sim 330$ nm) and RI detectors, the GPC traces (Fig. 1d) strongly confirmed that P(*t*BMA-*b*-DMA) chains have been covalently bonded with C_{60} molecules. It is possible that minute fractions of unreacted precursor may be present, and this small fraction is extremely difficult to remove due to the similar characteristics of both polymeric systems. The weight percentages of C_{60} and P(*t*BMA-*b*-DMA) were calculated by comparing its TGA curve with those of pure C_{60} and

P(*t*BMA-*b*-DMA), since C_{60} was stable above 600 °C. The molar ratio of C_{60} to P(*t*BMA-*b*-DMA) determined was close to 1:1, indicating that one polymer chain was grafted to only one C_{60}. UV-vis. absorption spectra of P(MAA_{102}-*b*-DMA_{67})-*b*-C_{60} in aqueous solutions at pH 3 show peaks at 256, 330, and 400 nm. These further confirmed that the grafting of the polymer to the C_{60}. The absorption spectra at pH 11, however, show continuous absorption in the 200 to 500 nm wavelength range. This may be attributed to the formation of the charge-transfer complex between the DMA units and C_{60} [19], which perturbed the localization of the conjugated bonds. The variation in absorption spectra with pH shows that the electronic environments around the C_{60} at pH 3 and 11 are due to the disparity in aggregation phenomena.

Visible light transmittance at a wavelength of 600 nm of P(MAA-*b*-DMAEMA)-*b*-C_{60} solution was measured from pH 2 to 12 to monitor the cloudy region as shown in Fig. 3. It is evident that between pH 5.4 and 8.8, the copolymer becomes insoluble due to complexation and overall charge neutralization near the isoelectric point (IEP)[28],[29]. This behavior is similar to that of P(MAA-*b*-DMAEMA) [29] and P(MAA-*b*-DEAEMA) [9] in solution. It can be concluded that the water-soluble C_{60} containing P(MAA-*b*-DMAEMA) retains the polyampholyte properties in solution. In addition, visible light transmittance of the solution measured at 55 °C shows that the pH of the insoluble region shifts slightly to between 5.2 and 8.4. This relative similarity of low- and high-temperature insoluble regimes is due to the intrinsic decrease of pH with increasing temperature and therefore indicates that the isoelectric point of the copolymer is not drastically affected by the temperature change.

Based on the above results, the stimuli-responsive behaviour of the well-defined and water-soluble C_{60}-containing block copolymer in solution is demonstrated. Next, we examined the solution behaviour of the copolymer with step-wise changes in pH for a complete understanding of pH-dependent association behavior in the soluble regions.

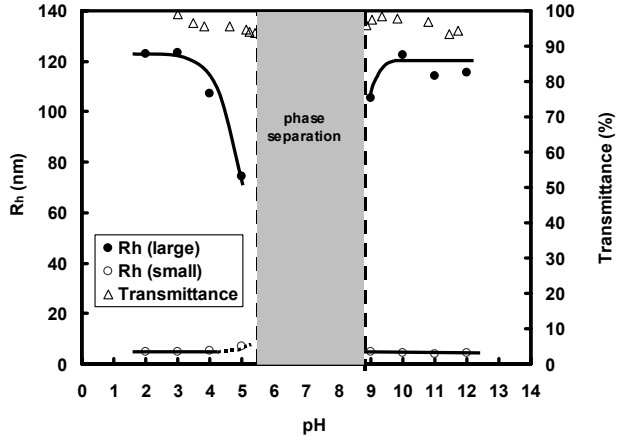

Fig. 3. pH dependence of R_h and visible light transmittance at 25 °C.

Dynamic light scattering was carried out as a function of pH. The hydrodynamic radii were obtained by applying the Stokes-Einstein relationship to decay rates and the pH dependence of R_h is shown in Fig. 3. At pH values lower than 5 and higher than 9, decay time distribution functions revealed two translational diffusion modes, while at moderate pH phase separation occurs and no light scattering was carried out (The experimental data from DLS are provided in supporting information). The average hydrodynamic radius of large particles remains constant at about 120 nm when the pH was increased from 2.0 to below 4.0. In this region, the PMAA segments are predominantly not dissociated because the pK_a of methacrylic acid (pK_a = 5.35) lies considerably above these pH values [29]. Similarly, the PDMAEMA segments are mostly protonated because the pK_b of PDMAEMA is at 8.00 [29]. Therefore, it can be concluded that in this pH range the copolymer microstructure is largely unaffected by any variation in pH. The average hydrodynamic radius of large particles also remained constant at about 120 nm as pH was increased from 9.0 to 12.0, where the PMAA segments are primarily dissociated while the PDMAEMA segments are mainly deprotonated. The copolymer microstructure in this pH range is also largely unaffected by pH change. We have therefore identified that the copolymer aggregation microstructure is, to a large degree, stable below and above the insoluble pH range, and that the charge neutralization effects become significant only when the solution pH is close to the phase-separated range. In accordance with our hypothesis of stable microstructure over large pH range, the average size of the small particles in the copolymer solution remains constant at 5 nm, which corresponds to monomeric polymer chains (or unimers). If the hydrophobicity of any segment changes or if electrostatic attraction becomes significant with changes in pH, unimers may cease to exist since they are maintained by the strong electrostatic repulsion between the positively-charged chains, which keeps individual unimer chains solvated in aqueous solution. If the hydrophobicity of PDMAEMA increases significantly, the decrease in the hydrophile-lipophile balance (HLB) will favor the formation of micelles or larger aggregates. If electrostatic attraction between positively-charged PDMAEMA and negatively-charged ionized PMAA becomes significant, the formation of electrostatic complexes will produce insoluble precipitates. This will impede the formation of freely-solvated unimers or cause a decrease in the size of aggregates [28]. The stability of unimer size is thus an indication of the stability of the copolymer microstructure.

In contrast to hydrodynamic radii stability below pH 4.0 and above pH 9.0, there is a slight drop in aggregate size at pH of ~ 4.0 and ~ 9.0, and a marked decrease near the insoluble range at pH 5.0. This phenomenon is attributed to the formation of charge complexes near this range as suggested by Gohy et al. [28]. As pH is increased to above 4.0, some of the MAA units are ionized and they form charge complexes with positively-charged protonated PDMAEMA. These insoluble complexes form parts of the hydrophobic core of the aggregates and cause a reduction

in size. Indeed, the occurrence of local insoluble complexes arises within (and possibly near) the pH range 4.5 to 10.4.

Based on the above findings for pH-dependent association behaviour, we selected pH 3 and pH 11 to investigate the aggregation behavior of P(MAA-*b*-DMAEMA)-*b*-C_{60} as a function of temperature because these pH values represent stable conditions in the low-pH and high-pH soluble ranges respectively. The aggregation behavior of P(MAA-*b*-DMAEMA)-*b*-C_{60} at pH 3 was investigated using DLS at 25 and 55 ^{o}C. At this pH, the decay time distribution function revealed two translational diffusion modes, as is evident from the q^2 dependence of the decay rate. The fast decay mode corresponds to an average hydrodynamic radius (R_h) of ~ 5 nm, while the slow decay mode corresponds to an average R_h of ~ 120 nm. The balance of hydrophobic attraction and electrostatic repulsion arising from positively-charged amine groups, which accounts for the association of P(MAA-*b*-DMAEMA)-*b*-C_{60}, gives rise to the slow diffusional mode of the aggregates. The hydrophobic interactions arise from two different kinds of domains; the first consists of C_{60} while the other comprises PMAA segments. Instead of forming simple core-shell-like micelles as in diblock P(MAA-*b*-DMAEMA) system, the aggregates possess a microgel-like structure with hydrophobic domains comprised of separate C_{60} and PMAA segments inter-connected by the charged hydrophilic PDMAEMA segments. The strong electrostatic repulsion also gives rise to the coexistence of unimers (fast decay mode) with these aggregates.

When the Stokes-Einstein relationship was applied to the decay time distribution at 55 ^{o}C, the hydrodynamic size distribution was nearly identical at both low and high temperatures. Large aggregates with an average radius of about 120 nm and unimers with an average radius of about 5 nm co-exist in solution. This indicates that no apparent transformation in microstructure occurs with increasing temperature. At this pH, the PMAA segments and C_{60} molecules remain hydrophobic within the temperature range while the PDMAEMA segments remain hydrophilic as they are fully protonated. In other words, the HLB of the copolymer is not adversely affected by the rise in temperature in this experimental range.

At pH 11, the decay time distribution function also shows two translational diffusion modes at 25 ^{o}C. The fast mode corresponds to an average hydrodynamic radius of ~ 5 nm, while the slow mode corresponds to an average radius of ~ 120 nm. The ionized $–COO^-$ and the deprotonated PDMAEMA segments are hydrophilic at this temperature, while the C_{60} is hydrophobic. Our previous work on PDMAEMA-*b*-C_{60} in aqueous solution at high pH revealed the formation of the charge-transfer complex between the PDMAEMA segments and C_{60} [19], which enhanced the solubility of C_{60} in water. In the formation of this complex, the lone pair electrons on the nitrogen act as the electron donor and C_{60} acts as the electron acceptor. Some of the C_{60} molecules aggregate with one another through hydrophobic interaction, while the others form the charge-transfer complex with PDMAEMA segments and they act as physical cross-linkers. Therefore, large particles are produced in solution coexisting with unimers by the combination of hydrophobic interactions, electrostatic repulsion and the charge-transfer interaction, which give rise to large aggregate complexes instead of simple core-shell-like micelles.

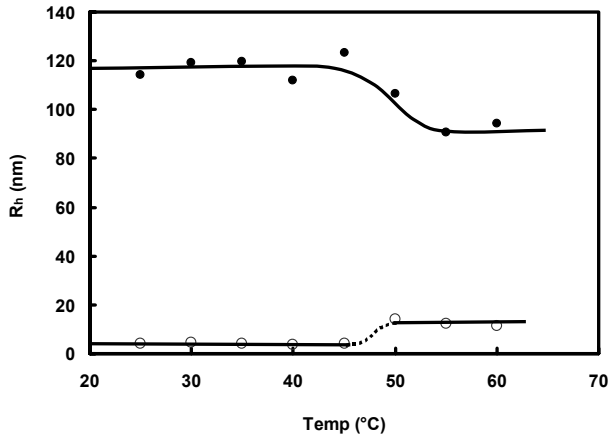

Fig.4 Temperature dependence of R_h values of P(MAA_{102}-*b*-$DMAEMA_{67}$)-*b*-C_{60} at pH 11

In contrast to the similarity of decay time distributions at pH 3, the difference in decay time distributions at 25 and 55 °C was apparent at pH 11. The temperature dependence of hydrodynamic radii is shown in Fig. 4. A gradual shift in hydrodynamic size distribution occurred as temperature was increased. Between 25 and 45 °C, unimers and aggregates co-exist with no change in unimer or aggregate size. At 50 °C and beyond, an intermediate translational diffusion mode appears, corresponding to a hydrodynamic radius of about 13 nm while the fast mode disappears. The aggregates were smaller in size, with an average radius of only about 90 nm. The appearance of the intermediate mode, disappearance of the fast mode, and decrease in aggregate R_h all occur between 45 and 50 °C. As temperature increases, hydrophilic PDMAEMA segments become hydrophobic [29]. Therefore, the C_{60} and PDMAEMA form a continuous hydrophobic domain at higher temperatures while PMAA is hydrophilic. This shift results in the tendency for micelle formation, with C_{60} and PDMAEMA comprising the hydrophobic core and ionized PMAA the hydrophilic shell. Whereas at low temperatures the hydrophilic PDMAEMA allows for unimer formation, the loss in hydrophilicity at higher temperatures causes micelles to form. The intermediate diffusion mode is thus attributed to micelles. Comparison with earlier studies on the properties of PDMAEMA and P(MAA-*b*-DMAEMA) block copolymers supports our hypothesis that the formation of micelles occur at elevated temperatures[28]. Lowe et al. found that the cloud point of a 1.0 w/v % DMAEMA homopolymer solution at pH 9.5 is in the range 32 to 46 °C depending on its molecular weight [29]. Therefore, at higher temperatures (in this case, at and above 50 °C) both C_{60} and PDMAEMA hydrophobicity induces the formation of core-shell micelles. The co-

existence of aggregates with micelles suggests that at higher temperatures, the combination of charge-transfer and hydrophobic interactions control the formation of these aggregates. The decrease in size of the aggregates can also be explained by the diminishing hydrophilicity of PDMAEMA, which tends to minimize its interaction with water molecules, resulting in denser hydrophobic domains and thus smaller aggregate size. The aggregates may also have larger aggregation numbers because of the decrease in HLB. The contribution to R_h from the increase in aggregation number is not as significant as the desolvation of PDMAEMA segments

The TEM micrographs revealed large aggregates with porous cores at pH 3 and at 25 °C, as shown in Fig. 5a. The cores of these aggregates are visibly less dense than those observed at pH 11 and at 25 °C (Fig. 5b), which have compact cores. This indicates that the aggregate microstructures are different from each other.

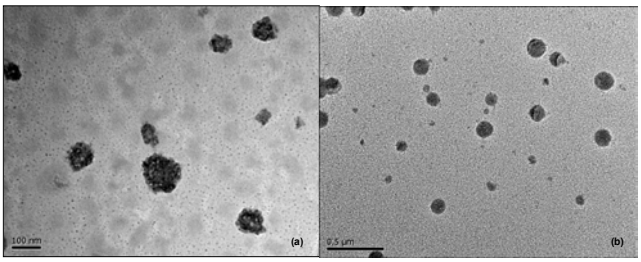

Fig. 5 TEM images of P(MAA_{102}-*b*-$DMAEMA_{67}$)-*b*-C_{60} aggregates formed in aqueous solution at pH 3 (a) and pH 11 (b).

A schematic representation of the aqueous microstructure of the copolymer is shown in Fig. 6. Three contrasting microstructures were deduced across the pH and temperature ranges examined in the present study. At pH 3 and at 25 °C, unimers with positively-charged PDMAEMA chains co-exist with aggregates comprising separate C_{60} and PMAA hydrophobic domains. At pH 11 and at 25 °C, unimers with negatively-charged ionized PMAA chains co-exist with aggregates consisting of C_{60} hydrophobic domains cross-linked due to charge-transfer interactions with PDMAEMA segments. The cross-linked cores proposed at this pH are compact cores of higher density than the porous cores hypothesized at pH 3. This is in agreement with the contrasting images visualized using the transmission electron microscope. At pH 11 and at 55 °C, micelles with a hydrophilic PMAA shell and a continuous hydrophobic C_{60} and PDMAEMA core co-exist with aggregates of reduced size. The association behaviour of the C_{60}-containing P(MAA-*b*-DMAEMA) copolymer contrasts with that of pure P(MAA-*b*-DMAEMA) of comparable composition. In the latter, smaller micelles and large hollow aggregates were formed below and above the IEP respectively at room temperature. The combination of electrostatic and hydrophobic interactions together with the minimization of chain-stretching of PDMAEMA blocks control the formation of these large hollow aggregates [28]. In the C_{60}-containing block copolymer, the combination of electrostatic and hydrophobic interactions and the presence of C_{60} as an additional hydrophobic group as well as a charge-transfer acceptor produce unimers and aggregates at low pH and at high pH at low temperatures and micelles and aggregates at high pH and at high temperatures

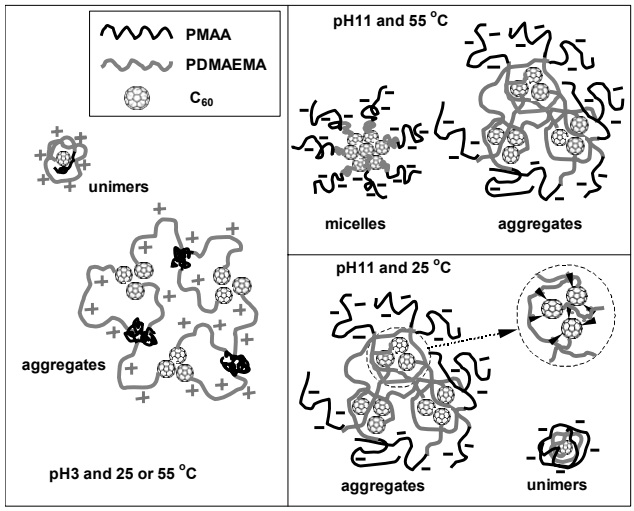

Fig. 6. Schematic representation of the possible microstructures of P(MAA_{102}-*b*-$DMAEMA_{67}$)-*b*-C_{60} in aqueous solutions at different pH and temperatures. The inset is the enlargement of the CT complex.

V. CONCLUSIONS

The well-defined and water-soluble C_{60}-containing amphiphilic block copolymer was synthesized by ATRP and its stimuli-responsive self-assembly behaviour was systematically characterized by DLS and TEM. P(MAA_{102}-*b*-$DMAEMA_{67}$)-*b*-C_{60} showed enhanced solubility in aqueous medium at room and elevated temperatures at low and high pH but was insoluble at intermediate pH. The co-existence of unimers and aggregates was observed at low and high pH. At elevated temperatures at high pH, however, micelles and aggregates co-exist. Hydrophobic and electrostatic interactions control the aggregate formation at low pH, while hydrophobic, electrostatic and charge- transfer interactions control the aggregate formation at high pH. Although P(MAA_{102}-*b*-$DMAEMA_{67}$)-*b*-C_{60} possesses similar polyampholyte properties as P(MAA_{102}-*b*-$DMAEMA_{67}$), the aggregation mechanism is totally different from that of P(MAA_{102}-*b*-$DMAEMA_{67}$).

ACKNOWLEDGMENT

We would like to thank the Singapore-MIT Alliance for providing financial support.

REFERENCES

[1] E. Nakamura, and A. Isobe, "Functionalized fullerenes in water. The first 10 years of their chemistry, biology, and nanoscience", *Acc. Chem. Res.*, *36*, 807-815, 2003.

[2] L.V. Vinogradova, E. Y. Melenevskaya, A. S. Khachaturov, E. E. Kever, L. S. Litvinova, A. V. Novokreshchenova, M. A. Sushko,

S. I. Klenin, and V. N. Zgonnik, "Water-soluble complexes of C-60 fullerene with poly(N-vinylpyrrolidone)", *Vysokomolekulyarnye Soedineniya Seriya A & Seriya B 40*, 1854-1862, 1998.

[3] D. V. Khonarev, and R. N. Lyubovskaya, "Donor-acceptor complexes and radical-ion salts based on fullerenes", *Uspekhi Khimii*, *68*, 23-44, 1999.

[4] L.Y. Chiang, J. B. Bhonsle, L. Wang, S. F. Shu, T. M. Chang, and J. R. Hwu, "Efficient one-flask synthesis of water-soluble [60]fullerenols", *Tetrahedron 52*, 4963-4972, 1996.

[5] M. Brettreich, and A. Hirsch, "A highly water-soluble dendro[60]fullerene", *Tetrahedron Lett*, *39*, 2731-2734, 1998.

[6] J. Adamov, M. V. Miloradov, "New materials on the basis of amino derivatives of fullerene C-60", Adv. Mater. Pros. Mater. Sci. forum, *282,* 101-107, 1998.

[7] S. Yamago, H. Tokuyama, E. Nakamura, K. Kikuchi, S. Kananishi, K. Sueki, H. Nakahara, S. Enomoto, and F. Ambe, F. "In-vivo biological behaviour of a water-misible fullerene –C-14 labeling, absorption, distribution, excretion and acute toxicity", *Chem. Biol. 2*, 385-389, 1995.

[8] Y. P. Sun, G. E. Lawson, W. J. Huang, A. D. Wright, and D. K. Moton, "Preparation and characterization of highly water-soluble pendant fullerene polymers", *Macromolecules 32*, 8747-8752, 1999.

[9] S. Dai, P. Ravi, K. C. Tam, B. W. Mao, and L. H. Gan, "Novel pH-responsive amphiphilic diblock copolymers with reversible micellization properties", *Langmuir 19*, 5175-5177, 2003.

[10] B. Sitharaman, S. Asokan, I. Rusakova, M. S. Wong, and L. J. Wilson, "Nanoscale aggregation properties of neuroprotective carboxyfullerene (C-3) in aqueous solution", *Nano Letters 4,*1759-1762, 2004.

[11] X. H. Wang, S. H. Goh, Z. H. Lu, S. Y. Lee, and C. Wu, "Light-scattering characterization of fullerene-containing poly(alkyl methacrylate)s in THF", *Macromolecules 32*, 2786-2788, 1999.

[12] T. Song, S. Dai, K. C. Tam, S. Y. Lee, and S. H. Goh, "Aggregation behavior of two-arm fullerene-containing poly(ethylene oxide)", *Polymer 44*, 2529-2536, 2003.

[13] T. Song, S. Dai, K.C. Tam, S. Y. Lee, and S. H. Goh, "Aggregation behavior of C-60-end-capped poly(ethylene oxide)s", *Langmuir 19*, 4798-4803, 2003.

[14] P. Zhou, G. Q. Chen, H. Hong, F. S. Du, Z. C. Li, and F. M. Li, "Synthesis of C-60-end-bonded polymers with designed molecular weights and narrow molecular weight distributions via atom transfer radical polymerization", *Macromolecules 33*, 1948-1954, 2000.

[15] F. Audouin, R. Nuffer, and C. Mathis, "Synthesis of di- and tetra-adducts by addition of polystyrene macroradicals onto fullerene C-6", *J. Polym. Sci.Part A Polym. Chem. 42,* 3456-3463, 2004.

[16] D. Yang, L. Li, and C. Wang, "Characterization and photoconductivity study of well-defined C-60 terminated poly(tert-butyl acrylate-b-styrene)", *Mater. Chem. Phys. 87,* 114-119, 2004.

[17] J. Yang, L. Li, and C. Wang, "Synthesis of a Water Soluble, Monosubstituted C_{60} Polymeric Derivative and Its Photoconductive Properties", *Macromolecules 36*, 6060-6066, 2003.

[18] C. H. Tan, P. Ravi, S. Dai, and K. C. Tam, "Polymer-Induced Fractal Patterns of [60]Fullerene Containing Poly(methacrylic acid)", in Salt Solutions *Langmuir 20,* 9901-9904, 2004.

[19] S. Dai, P. Ravi, C. H. Tan, and K. C. Tam, "Self-Assembly Behavior of a Stimuli-Responsive Water-Soluble [60]Fullerene-Containing Polymer", *Langmuir 20,* 8569-8575, 2004.

[20] X. M. Liu, and L. S. Wang, "A one-pot synthesis of oleic acid end-capped temperature- and pH-sensitive amphiphilic polymers", *Biomaterials 25*, 1929-1936, 2004.

[21] M. Rackaitis, K. Strawhecker, and E. Manias, "Water-soluble polymers with tunable temperature sensitivity: Solution behavior", *J. Polym. Sci. Part B: Polym. Phys. 40*, 2339-2342, 2002.

[22] A. Kikuchi, and T. Okano, "Pulsatile drug release control using hydrogels", *Adv. Drug Deliv. Rev. 54*, 53-57, 2002.

[23] T. Saitoh, Y. Suzuki, and M. Hiraide, "Preparation of poly(N-isopropylacrylamide)-modified glass surface for flow control in microfluidics", *Anal. Sci.*, *18*, 203-205, 2002.

[24] I. Roy, and M. N. Gupta, "Smart polymeric materials: Emerging biochemical applications", *Chem. Biol. 10*, 1161-1171, 2003.

[25] Y. H. Ma, Y. Q. Tang, N. C. Billingham, S. P. Armes, and A. L. Lewis, "Synthesis of biocompatible, stimuli-responsive, physical gels based on ABA triblock copolymers", *Biomacromolecules 4*, 864-868, 2003.

[26] Y. Q. Tang, S. Y. Liu, S. P. Armes, and N. C. Billingham, "Solubilization and controlled release of a hydrophobic drug using novel micelle-forming ABC triblock copolymers", *Biomacromolecules 4*, 1636-1645, 2003.

[27] M. Torres-Lugo, M. García, and R. Record, and N. A. Peppas, "Physicochemical behavior and cytotoxic effects of p(methacrylic acid-g-ethylene glycol) nanospheres for oral delivery of proteins", *J. Controlled Release 80*, 197-205, 2002.

[28] J. F. Gohy, S. Creutz, M. Garcia, B. Mahltig, M. Stamm, and R. Jérôme, "Aggregates formed by amphoteric diblock copolymers in water", *Macromolecules 33*, 6378-6387, 2000.

[29] A. B. Lowe, N. C. Billingham, and S. P. Armes, "Synthesis and characterization of zwitterionic block copolymers", *Macromolecules 31*, 5991-5998, 1998.

[30] H. Okamura, K. Miyazono, M. Minoda, K. Komatsu, T. Fukuda, and T. Miyamota, "Synthesis of highly water soluble C-60 end-capped vinyl ether oligomers with well-defined", *J. Poly. Sci. A Poly. Chem., 38*, 3578-3585, 2000.